

A Study on Fluctuating Pressure Load on High Speed Train Passing through Tunnels

Sung-II Seo*

*Conventional Rail Division, Korea Railroad Research Institute,
360-1 Woulam-Dong, Uiwang City, Kyonggi-Do 437-757, Korea*

Choon-Soo Park

*High Speed Rail Division, Korea Railroad Research Institute,
360-1 Woulam-Dong, Uiwang City, Kyonggi-Do 437-757, Korea*

Oak-Key Min

*Department of Mechanical Engineering, Yonsei University,
Seoul 120-749, Korea*

The carbody structure of a high speed train passing through a tunnel is subjected to pressure fluctuation. Fatigue strength of the carbody structure against the fluctuating pressure loading should be proved in the design stage for safety. In this study, to get the useful information on the pressure fluctuation in the tunnel, measurement has been conducted during test running of KHST on the high speed line for two years. The measured results were analyzed and arranged to be used for carbody design. A prediction method for the magnitude and frequency of pressure change was proposed and the propagating characteristics of pressure wave was investigated. By statistical analysis for the measured results, a pressure loading spectrum for the high speed train was given. The proposed method can also be used to estimate the pressure loading spectrum for new high speed line at design stage combined with the results of train performance simulation.

Key Words : Fluctuating Pressure, High Speed Train, Loading Spectrum, Measurement System, Pressure Wave, Train Performance Simulation, Tunnel

Nomenclature

<p>A : Sectional area of train</p> <p>A_t : Sectional area of tunnel</p> <p>L : Length of tunnel</p> <p>L_i : Encountering location of train with entry pressure wave ($i=0, 1, 2, 3$)</p> <p>L'_i : Encountering location of train with tail pressure wave ($i=0, 1, 2, 3$)</p> <p>L_{tr} : Length of train</p> <p>$f(\Delta p)$: Probability density function</p>	<p>n : Wave reflecting odd number (1, 3, 5, 7, ...)</p> <p>Δp : Pressure change</p> <p>ΔP_1 : Maximum pressure change</p> <p>ΔP_2 : Second pressure change</p> <p>ΔP_{mit} : Initial pressure rise</p> <p>t_i : Encountering time of train with entry pressure wave ($i=0, 1, 2, 3$)</p> <p>t'_i : Encountering time of train with tail pressure wave ($i=0, 1, 2, 3$)</p> <p>V : Entrance train velocity in km/h</p> <p>V_i : Critical encountering velocity in km/h</p> <p>V_p : Sound velocity</p>
---	---

* Corresponding Author,

E-mail : siseo@krri.re.kr

TEL : +82-31-460-5623; **FAX :** +82-31-460-5699

Conventional Rail Division, Korea Railroad Research Institute, 360-1 Woulam-Dong, Uiwang City, Kyonggi-Do 437-757, Korea. (Manuscript **Received** August 25, 2005; **Revised** February 10, 2006)

1. Introduction

With the opening of KTX (Korea Train eXpress), social concerns on the high speed train have in-

creased and demands for safety and comfortability also have increased. Particularly, when a high speed train enters a tunnel, impulse pressure wave is generated by the sudden change of the flow field around the entrance. It is propagated into the tunnel. Rapid pressure change in the cabin by the external pressure wave can cause ear ringing of the passenger, which is the major uncomfortable factor in the high speed train. The advanced high speed train systems adopt the various countermeasures for the pressure change in the cabin. In case of KTX, the on-board automatic train control system receives the sign from the ground signal emitter before the tunnel and closes the flaps of the air ventilation system. Airtightness is maintained while the train passes through the tunnel. In case of KHST (Korea High Speed Train), next generation high speed train developed by homegrown technologies, whenever the sensors in the cabin detect the pressure change, the pressurization system operates and compensates actively the pressure change. The pressure control systems are effective on keeping comfortability in the cabin, however it causes the carbody structure to burden another load. The carbody structure is subjected to external loading generated by the pressure difference between the cabin and the tunnel. Especially, since three quarter of our country is mountainous area, tunnels are indispensably constructed to make a straight line. As the result, the safety of the carbody structure subjected to fluctuating external pressure should be secured. In addition, KHST is made of aluminum alloys for weight reduction which is different from KTX. The welded joints on the aluminum carbody structure is susceptible to defects such as porosity and hot crack, which significantly reduce the fatigue strength (Seo, 2002). In France, the most part of the high speed line is on the flat ground and pressure fluctuation in the tunnel doesn't cause a serious problem. So, researches on the tunnel problems haven't been active. However, Japanese researchers have been much interested in these tunnel problems. The natural environment of Japan is similar to that of Korea. Japanese country is full of mountains, so Shinkansen Line should run through many tunnels. The carbody structure

of Shinkansen is also made of aluminum alloys and susceptible to fatigue failure. Japanese researchers have studied the phenomenon related to the tunnel to construct the safe and reliable high speed railway system. The research themes are mainly focused on the flow field analysis for the high speed train in the tunnel. Computational fluid dynamic analysis on the tunnel flow was conducted and the results were compared with the experimental results (Ogawa, 1994). However, researches on the effect of tunnel flow on the carbody structure were rare.

Nihei et-al conducted experimental studies on the pressure fluctuation in the tunnel to assess the fatigue strength of Shinkansen aluminum carbody structure and presented the data on the pressure range and frequency (Nihei, 1998). However, detailed information on the pressure increase caused by the encountering train in the tunnel and the attenuation of incident pressure at the tunnel boundary is not sufficient. Also, because the pressure fluctuation depends on the tunnel dimension and the nose shape of carbody, the foreign tunnel data is not appropriate to be used in Korean high speed railway system. Domestic researchers conducted the numerical study on the tunnel impulse pressure. Kwon et-al studied the unsteady compressible flow field induced by a high speed train passing through a tunnel (Kwon, 2002). Nam studied the pattern of pressure wave in tunnel (Nam, 2004). The previous studies were focused on analysis of flow field and pressure wave. They don't provide sufficient information on the effect of pressure wave on the fatigue failure of the carbody structure.

In this study, measurement of pressure fluctuation in the tunnel has been conducted during test running of KHST on the high speed line for two years. The measured results were analyzed and arranged to get the appropriate information for evaluation of fatigue strength of carbody structure. A prediction method for the magnitude and frequency of pressure fluctuation was proposed and the propagating characteristics of pressure wave was investigated. The pressure increase generated by the opposite train was also measured and assessed statistically. Based on the analyzed

data, a method to predict the pressure loading on the carbody was presented with the combination of the train performance simulation method.

2. Pressure Wave in Tunnel

2.1 Generation and propagation of pressure wave

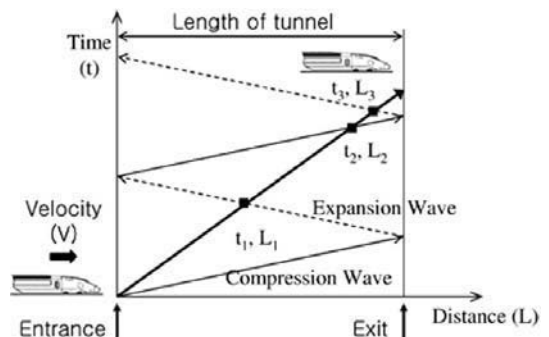
When a high speed train enters a tunnel as shown in Fig. 1, entry compressive pressure wave is generated by the sudden change of air flow around the front of carbody. This entry pressure wave propagates into the tunnel at the speed of sound. When it reaches the end, some portion of wave energy is dissipated around the exit and the other portion is reflected into the tunnel in the form of expansion wave. The dissipated wave energy is also radiated in the form of micro-pressure wave. It is called tunnel sonic boom and damages the residents near the tunnel. The reflected expansion wave is reflected again and converted into the compression wave at the entrance. The reflection and propagation process is repeated as shown in Fig. 2 (Nam and Kwon, 2004). When the tail of the train enters the tunnel, expansion wave is generated and transmitted to the exit. The propagation process of the tail expansion wave is the same as that of the entry compression wave. Whenever the moving train encounters the different pressure wave, it experiences pressure fluctuation. Encountering times and locations of the moving train with the pressure wave



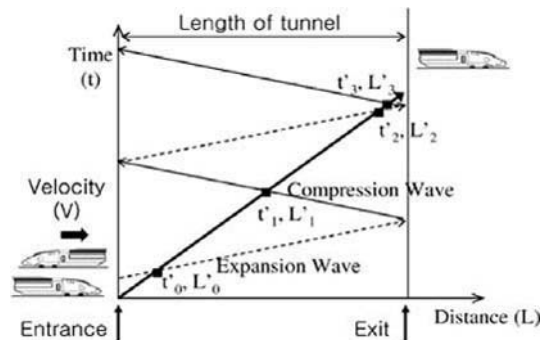
Fig. 1 Korea High Speed Train passing through a tunnel

are shown in Fig. 2. The first encountering time with the nose (or entry pressure wave) is denoted as t_0 and the location is denoted as L_0 . The encountering times and locations with the reflected waves are denoted in sequence. On the other hand, the first encountering time with the tail pressure wave is denoted as t'_0 and the location is denoted as L'_0 .

For the passengers in the cabin not to feel ear ringing caused by the pressure fluctuation, the carbody is kept airtight and actively pressurized. Figure 3 shows the difference of pressure fluctuation between the interior and the exterior of the cabin. The times shown in Fig. 2 are marked in Fig. 3. They indicate the pressure rise and drop time in time sequence. The first entry compression wave is dropped at time t_0 by the following expansion wave caused by the tail. The next reflected expansion wave caused by the nose drops the pressure at time t_1 . The succeeding reflected compression wave caused by the tail raises the pressure at time t'_1 . In this way, the pressure



(a) Pressure wave generated by nose



(b) Pressure wave generated by tail

Fig. 2 Pressure fluctuating process in tunnel

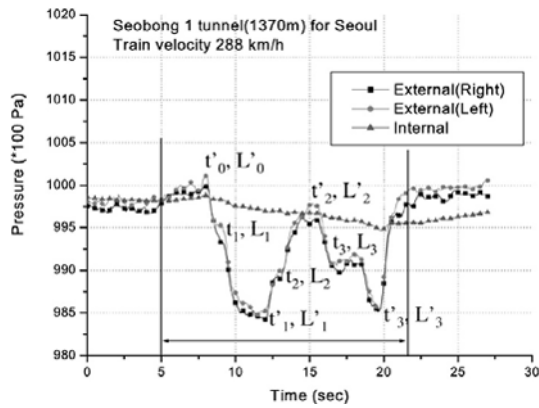


Fig. 3 Difference of pressure fluctuation between interior and exterior of cabin (absolute pressure)

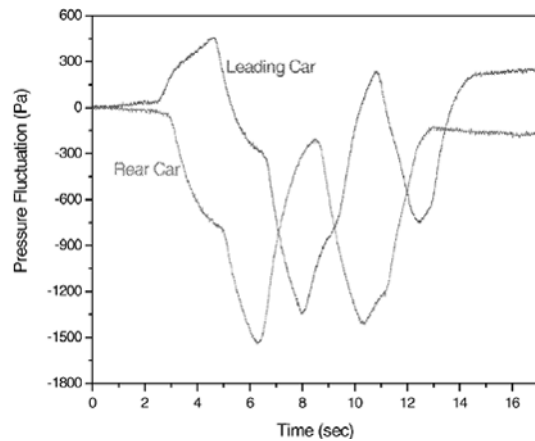


Fig. 4 Pressure fluctuating history in leading and rear car

fluctuating points shown in Fig. 3 are related with the times defined in Fig. 2. Figure 3 shows that the pressure fluctuation of the interior is negligible compared with that of the exterior. The carbody structure undergoes pressure loading corresponding to the external pressure fluctuation.

2.2 Pressure fluctuating patterns

Pressure fluctuation is caused by the pressure waves generated by the nose and the tail of the high speed train entering the tunnel as shown in Fig. 2. Figure 4 shows the examples of pressure wave pattern in the tunnel. The leading car genera-

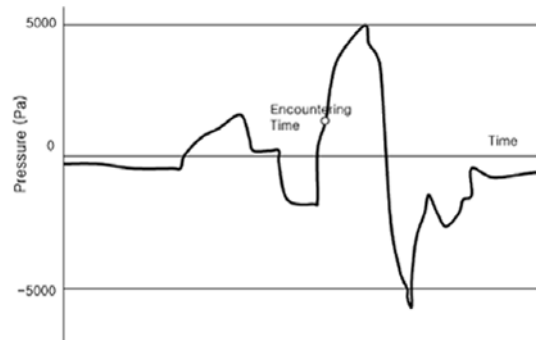
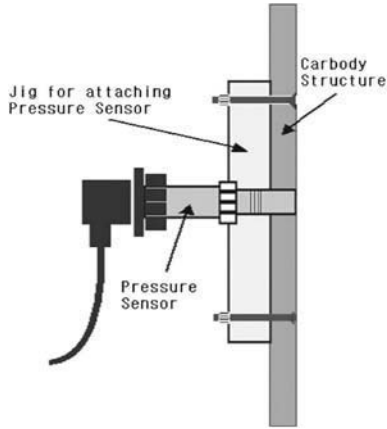


Fig. 5 Pressure increase caused by encountering train

tes compression wave first, but the rear car (or tail car, last car) generates expansion wave first. When the train encounters the opposite train in the tunnel, another pressure fluctuation is caused by the pressure waves of the opposite train. Figure 5 shows the typical pressure fluctuating pattern of the encountering case. The pressure is drastically raised at the encountering moment. In other words, the encountering moment is just before the peak point shown in Fig. 5. The pressure loading on the carbody is the combination of these pressure fluctuations.

3. Testing Method and Measurement System

To investigate systematically the pressure fluctuation around the high speed train in the tunnel, pressure sensors were installed on the cabin and the carbody. Pressure was measured while KHST was running on Seoul-Busan high speed line. The pressure sensor was fixed to the outer skin of the carbody by the jig as shown in Fig. 6. In the cabin, the pressure sensor was installed 1 meter above the floor. The measurement system to analyze the physical data was constructed on board as shown in Fig. 7. The voltage signal transmitted from the pressure sensor is converted into the physical quantity on the measurement system and displayed on the monitor in real time following the process of Fig. 8. Velocity and travelling distances were also measured and all the measured data are recorded in the hard disk. After mea-



(a) Jig to fix pressure sensor



(b) Pressure sensor on skin of carbody

Fig. 6 Pressure sensor and fixing jig



Fig. 7 Data acquisition and analysis system

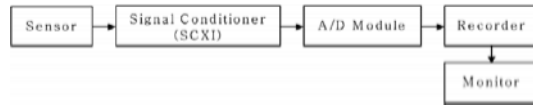


Fig. 8 Process to transmit pressure signal

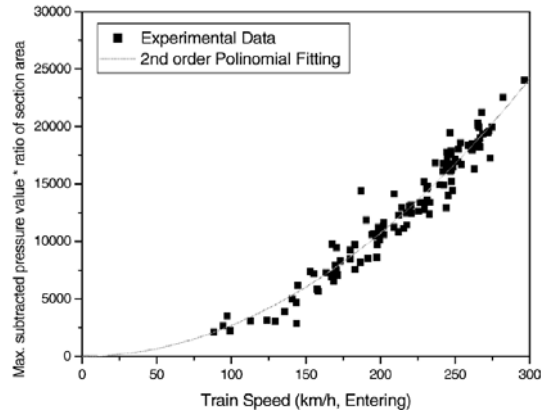


Fig. 9 Polynomial fitting between train velocity and maximum pressure change (KHST)

urement was completed, the data were processed and analyzed.

4. Testing Results and Investigation

4.1 Pressure change in independent running

To get the relation between train velocity and pressure fluctuation when a high speed train enters the tunnel independently, the measured data were analyzed. It was known that the entry compression wave is proportional to the velocity square and the area ratio of train and tunnel (Nihei, 1998). The entrance velocities and corresponding maximum pressure changes were plotted on the graph. Figure 9 shows the relation between maximum pressure change and velocity. The vertical axis of Fig. 9 is defined as $\Delta P_1 \times \left(\frac{A_t}{A}\right) (N)$. The polynomial regression analysis result for Fig. 9 shows that the maximum pressure change is expressed by the following equation.

$$\Delta P_1 = 0.2684 V^2 \left(\frac{A}{A_t}\right) \text{ for KHST} \quad (1)$$

The tunnel area of Seoul-Busan high speed line A is 107 m² and the sectional area of KHST A_t is 10.2 m².

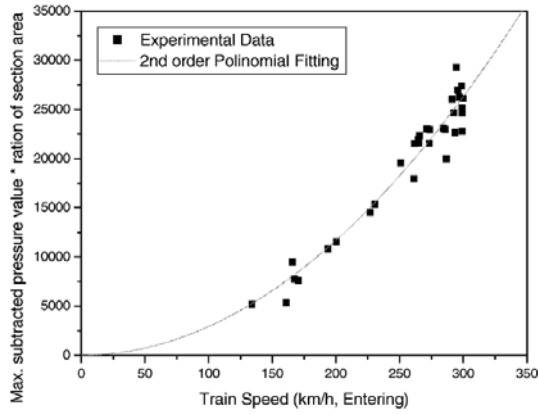


Fig. 10 Polynomial fitting between train velocity and maximum pressure change (KTX)

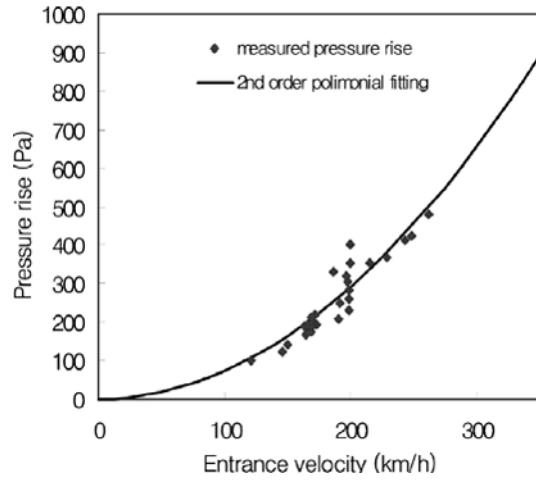


Fig. 12 Relation between pressure rise and entrance velocity

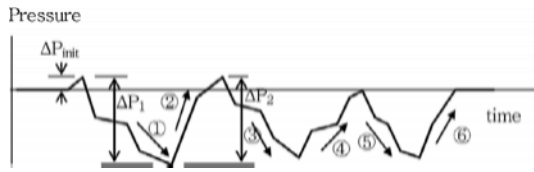


Fig. 11 Definition of pressure rise, pressure change and cycle

For the other high speed train KTX, the same process was applied. The measured results were plotted on Fig. 10. They are expressed by the following equation (2).

$$\Delta P_1 = 0.2916 V^2 \left(\frac{A}{A_t} \right) \text{ for KTX} \quad (2)$$

The difference of the coefficients in Eqs. (1) and (2) indicates the difference of the front shapes of two high speed trains.

4.2 Pressure rise in entering a tunnel

Just after the train enters the tunnel, initial pressure rise happens due to change of air flow. Figure 4 shows the pressure rise caused by the leading car. However, when the tail enters the tunnel, pressure rise doesn't happen. Only pressure fluctuation by compression and expansion wave is generated. The pressure rise is defined in Fig. 11. To find a simple equation for the pressure rise, the measured results were analyzed as shown in Fig. 12. It can be expressed by the following equation.

$$\Delta P_{init} = 0.07653 V^2 \left(\frac{A}{A_t} \right) \quad (3)$$

4.3 Pressure increase caused by encountering train

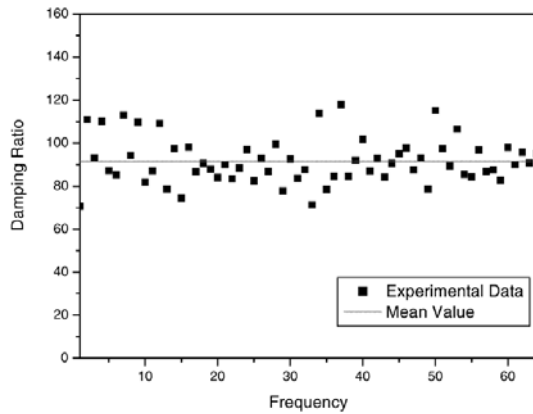
When the train encounters an opposite train in the tunnel, the pressure wave generated by the opposite train is superposed. Pressure fluctuation is increased by the encountering train as shown Fig. 5. Since the magnitude of the increase depends on encountering time, location and relative velocity, lots of measured data are required to induce the exact relation. During test running of KHST, encountering cases in the tunnel were limited. The measured data for increase of pressure fluctuation caused by the encountering train are summarized in Table 1. The average increase rate shown in Table 1 is 1.97 and the standard deviation is 1.01.

4.4 Attenuation of pressure at tunnel exit

The entry compression wave is propagated and reflected at the exit, where some wave energy is transmitted outdoors and dissipated. The reflected pressure wave is also propagated and encountered with the train. The recorded pressure fluctuation histories in the train were analyzed. The second pressure change attenuated by reflection was compared with the first pressure change defined in Fig. 11. The ratios of their absolute values were

Table 1 Pressure increase by encountering train

Tunnel	Entrance Velocity (km/h)	Maximum Pressure Change		
		Single Running (Pa)	Encountering (Pa)	Increasing rate
Tunnel No.4 (Seobong 1)	270.3	1869	1962	1.05
	287.4	2113	2155	1.02
Tunnel No.7 (Yongwa)	207.6	1103	3459	3.14
	210.8	1137	2982	2.62
	226.4	1312	3260	2.49
	274.6	1929	2066	1.07
Tunnel No.9 (Godeung)	297.5	2265	3789	1.67
Tunnel No.10 (Unju)	298.9	2286	3745	1.64
	202.5	1049	2170	2.07
	237.7	1146	1632	1.13
	271.0	1879	2160	1.15
	274.1	1922	3111	1.62
Tunnel No.11 (Nojang1)	147.5	557	1313	2.36
Tunnel No.15 (Sangbong 2)	135.7	471	2159	4.58

**Fig. 13** Distribution of attenuation ratio

calculated. Total 64 pressure fluctuation curves were investigated and the attenuation ratio of each pressure curve was calculated as shown in Fig. 13. The damping ratio shown in Fig. 13 is defined by the following equation.

$$\text{Damping Ratio (\%)} = \frac{\Delta P_2}{\Delta P_1} \times 100 \quad (4)$$

The mean ratio was 0.92 (=92%) and the standard deviation was 0.106.

4.5 Counting of pressure change in tunnel

The encountering frequency of pressure wave depends on the length and velocity of train and the length of tunnel. The encountering number of the train with the nose entry compression wave is determined by the propagation velocity of pressure wave and sound velocity regardless of tunnel length when the velocity of train exceeds a certain limit as shown in Fig. 2(a). However, the encountering number of the train with the tail entry expansion wave depends on the length of tunnel and train.

First, the critical encountering velocity with the nose entry compression wave is calculated by the reflecting times at tunnel exit referring to Fig. 2(a) as follows ;

$$V_n = \frac{V_p}{n} \quad (5)$$

Next, the critical encountering velocity with the tail entry expansion wave can be calculated by the following equation referring to Fig. 2(b).

$$V_n = \frac{V_p}{n} \left(1 - \frac{L_{tr}}{L} \right) \quad (6)$$

The number of pressure change is important to the fatigue strength of carbody. The pressure drop from the peak to the valley defined in Fig. 11 is counted as half load cycle according to the rain flow counting method. Pressure drop or rise less than 500 Pa is disregarded because the altitude of the line or the environmental condition can cause pressure change up to 500 Pa. Two typical pressure fluctuating patterns classified by the critical velocity are shown in Fig. 14. Whenever the train encounters the propagating pressure wave, the tunnel pressure is varied. When the sound velocity is 339 m/s(=1229 km/h) and reflecting number 5, the critical encountering velocity is calculated as 244 km/h(=1229/5). In case that the velocity of train is below 244 km/h deduced from Eq. (5), pressure change occurs six times as shown

in Fig. 14. In case that the train velocity is greater than 244 km/h, pressure change occurs four times.

4.6 Effect of critical tunnel length

When a train passes through a short tunnel, it is subjected to abnormal pressure fluctuation. The abnormal pressure fluctuating pattern is caused by the delayed tail expansion wave. Figure 15 shows the pressure wave pattern in the short tunnel, where the tail expansion wave can't encounter the train enough to make the normal pressure fluctuating pattern. If the tail expansion wave encounter the train two times in the tunnel, the normal pressure fluctuating pattern can be formed. The critical tunnel length is calculated by the following equation.

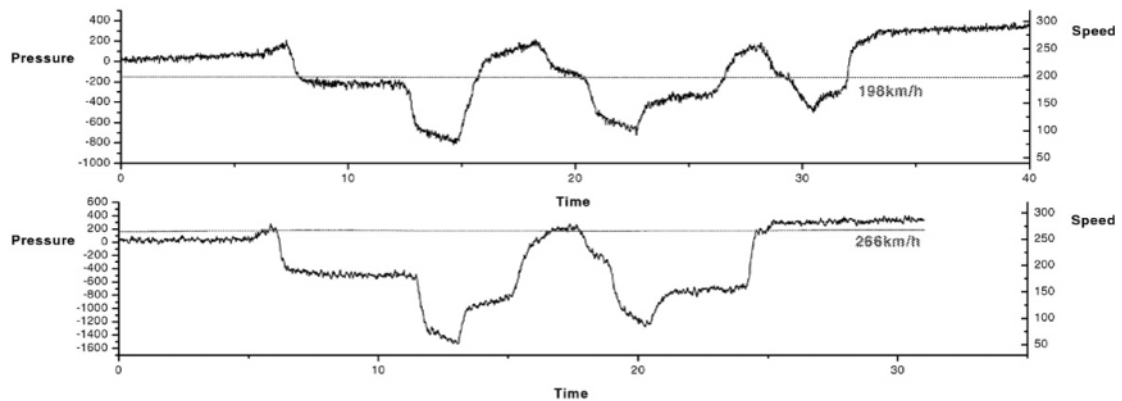


Fig. 14 Patterns of pressure fluctuation classified by critical velocity

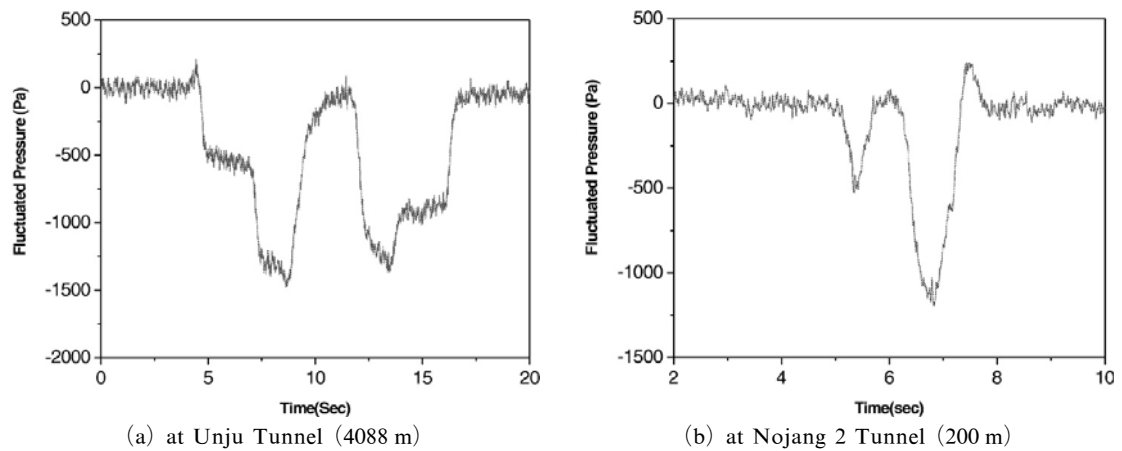


Fig. 15 Shape of pressure fluctuation

$$L_{cr} = \frac{L_{tr}}{V_p - 3V} V_p \quad (7)$$

In the short tunnel, the magnitude of the entry compression wave becomes less and the propagation and reflection is influenced greatly by the boundary effect. When the prototype KHST runs at the speed of 120 km/h, the critical tunnel length is calculated as 200 m. Below the critical length, the number of pressure change becomes 2, because the first pressure change is less than 500 Pa and negligible. The maximum pressure fluctuation is given by Eq. (8) based on the measured results.

$$\Delta P_1 = 0.2062 V^2 \left(\frac{A}{A_t} \right) \quad (8)$$

5. Pressure loading Spectrum for High Speed Line

5.1 Probability density function for pressure loading spectrum

To design a carbody against the fluctuating pressure loading, the distribution and frequency of the loading must be known. While KHST ran on the high speed line for reliability test, the pressure fluctuation in the tunnel was measured and recorded. The pressure changes defined in Fig. 11 were calculated and counted using the recorded pressure fluctuating histories. Table 2

Table 2 Frequency of pressure change in tunnels on high speed line

Pressure grade (Pa)	Number of pressure change in test running									
	1	2	3	4	5	6	7	8	9	10
975	13	30	25	15	33	43	35	8	10	15
1125	10	33	20	20	30	20	15	10	15	35
1275	3	35	10	18	28	40	25	10	10	15
1425	15	25	33	20	18	15	23	15	15	35
1575	15	18	18	15	20	33	20	23	15	10
1725	25	20	23	15	30	23	28	23	28	25
1875	13	13	25	18	10	30	20	20	20	10
2025	20	15	20	10	5	18	18	30	18	15
2175	25	13	8	15	5	3	18	25	15	20
2325	15	15	23	30	10	3	8	23	13	20
2475	23	13	15	23		3	5	8	8	10
2625	18	8	10	8	3	5	13	8	8	10
2775	13	8	13	15			3	15	10	5
2925	15	8	15	10			3	5	5	5
3075	15	5	13	8				3	5	5
3225	8	8	10						5	
3375		3		3					5	5
3525		3								5
3675										5
3825										
3975										
4125								3		
4275										
4425										
4575										
4725								3		

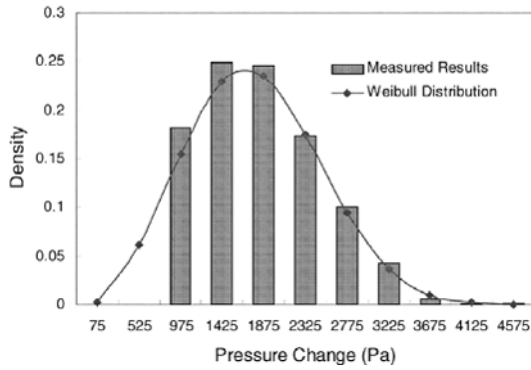


Fig. 16 Statistical analysis of pressure change

shows the arranged result for each route. For statistical analysis, the grade of pressure change is defined and each result is summed. The number of pressure change of a grade is summed totally to give the frequency. Figure 16 shows the distribution and frequency of each grade, where density is the frequency divided by the whole fluctuating times. The histogram originated from Table 2 is fitted by the well known Weibull distribution function. It is given by the following Eq. (9).

$$f(\Delta p) = \frac{2.7}{2000} \left(\frac{\Delta p}{2000} \right)^{1.7} \exp \left\{ - \left(\frac{\Delta p}{2000} \right)^{2.7} \right\} \quad (9)$$

Eq. (9) expresses the fraction of each pressure change for the specific route. It can be used as a pressure loading spectrum for the carbody of high speed train.

5.2 Estimation of pressure loading spectrum

In designing an advanced high speed train for new high speed line, the above pressure loading spectrum can't be applied because maximum running velocity, train performance or tunnel data is changed. A reasonable pressure loading spectrum is needed to design a carbody on the new line against fatigue failure. In this study a method to estimate the pressure loading spectrum is proposed.

The procedure to calculate the pressure loading spectrum based on the above results is presented in Fig. 17. After the design for a new line is finished, the detailed information of the line such as stations, curves, gradients and tunnels is

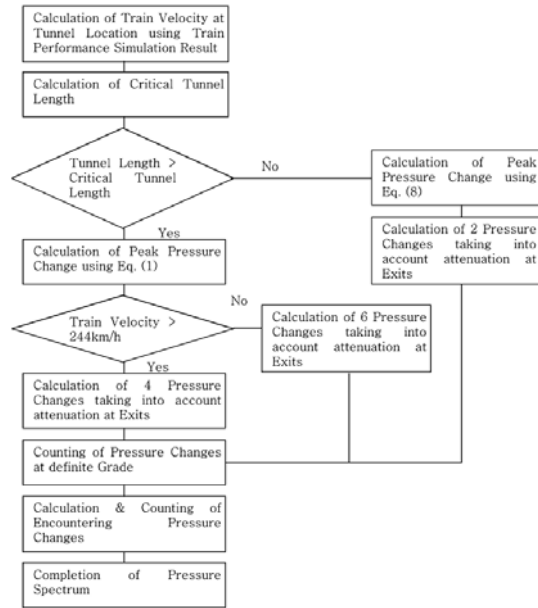


Fig. 17 Procedure to calculate pressure loading spectrum

known. The resistance of the train on the line is estimated by using the design formula (Lee, 2003). The simulation software TPS (Train Performance Simulation) can predict the traction power, the arrival time at each station, the train velocity and the consumed energy (Lee, 2004), based on the line data and the estimated resistance. TPS also requires the information on the weight of the train, the supplied power from the catenary and the on-board traction system. TPS calculates the balanced velocity and location of the train on the line. For example, the simulated performance of KHST on Seoul-Busan high speed line is shown in Fig. 18, where the design line data from Taegye to Busan under construction is used. KHST starts Seoul or Busan at the interval of 10 minutes and it runs at the maximum speed of 350 km/h. The velocity of train at each kilometer post and the encountering location with the opposite train is known by Fig. 17. Each line in Fig. 17 indicates the path of a train. The crossing points of each line with the opposite line group are the encountering points. KHST encounters the opposite train 36 times during a round trip. Among the encountering points, 16 points are the tunnel locations.

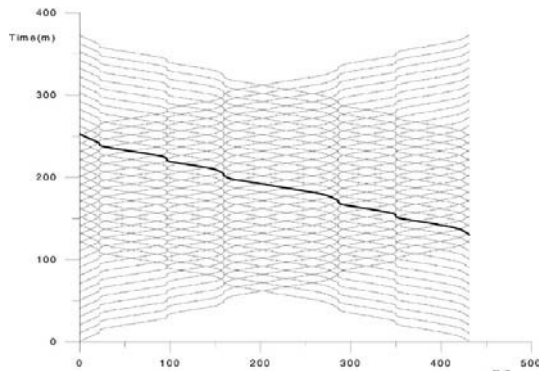


Fig. 18 Diagram of TPS result for new Seoul-Busan high speed line

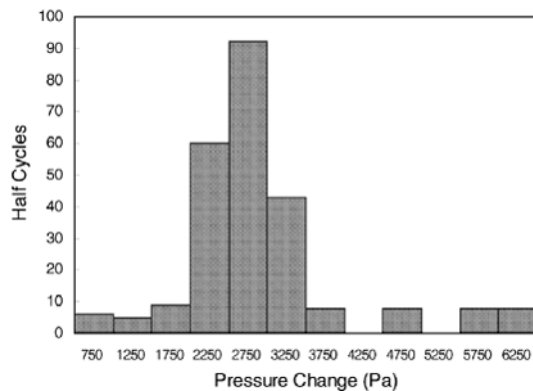


Fig. 19 Pressure loading spectrum for new Seoul-Busan high speed line

The pressure loading spectrum for KHST running on Seoul-Busan high speed line could be obtained by the procedure shown in Fig. 18. It is shown in Fig. 19. The tunnel data of new Seoul-Busan high speed line is used for train performance simulation.

6. Conclusions

The high speed train undergoes the pressure loading generated by the compression and expansion wave while passing through a tunnel, which affects the fatigue strength of carbody. Because the aluminum carbody structure is weak in fatigue strength, it should be designed against fluctuating loads. In this study, the fluctuating pressure around the high speed train in the tunnel was measured for design of the carbody. The

results were analyzed statistically and a useful spectrum function was proposed. A procedure to estimate the pressure loading spectrum at design stage was also proposed. The obtained results can be summarized as follows ;

(1) The maximum pressure change has definite relation with the entry velocity of the train. The coefficient in the formula for the maximum pressure change depends on the front shape of the train.

(2) Pressure increase added by the encountering train is about 1.9 times the maximum pressure change generated by the single train.

(3) Pressure wave is reflected at the tunnel exit and its magnitude is attenuated. The average attenuation ratio is 92%.

(4) The number of pressure change while passing a tunnel is counted by the rain flow counting method. When the train velocity is above 244 km/h, it is 4. Below 244 km/h, it is 6.

Acknowledgments

This study is the part of the project for development of Korea High Speed Train supported by Korea Ministry of Construction and Transportation.

References

- Kwon, H. B., Kim, T. Y., Kwon, J. H., Lee, D. H. and Kim, M. S., 2002, "The Numerical Simulation of the Pressure Wave for G7 Test Train in the Tunnel," *Journal of the Korean Society for Railway*, Vol. 5, No. 4, pp. 260~266.
- Lee, T. H., Park, C. S. and Shin, J. R., 2003, "Train Performance Simulation Program for Korea High Speed Railway System," *Journal of the Korean Society for Railway*, Vol. 6, No. 2, pp. 100~107.
- Lee, T. H., Park, C. S. and Shin, J. R., 2004,, "Train Performance Simulation and Evaluation for Kore High Speed Train," *Journal of the Korean Society for Railway*, Vol. 7, No. 2, pp. 120~124.
- Nam, S. W. and Kwon, H. B., 2004, "Theo-

retical x-t Diagram Analysis on Pressure Waves of High Speed Train in Tunnel,” *Journal of the Korean Society for Railway*, Vol. 7, No. 3, pp. 200~207.

Nam, S. W., 2004, “A Study on the Characteristics of Internal and External Pressure Variation for KTX,” *Journal of the Korean Society for Railway*, Vol. 7, No. 1, pp. 26~31.

Nihei, K., Ono, H., Koe, S. and Inamura, F., 1998, “Fatigue Strength Assessment Method for Shinkansen Aluminum Car Body Structures,”

Kawasaki Engineering Review, Vol. 138, pp. 30~39.

Ogawa, T. and Fujii, K., 1996, “Numerical Simulation of Compressible Flows Induced by a Train Moving into a Tunnel,” *Computational Fluid Dynamics Journal*, Vol. 3, No. 1, pp. 63~82.

Seo, S. I., 2002, “Studies on the Prevention of Damages on the Carbody of Aluminum Rolling Stocks,” *Journal of the Korean Society for Railway*, Vol. 5, No. 3, pp. 181~186.